

Interaction of Polar Molecules with Resonant Radio Frequency Electric Fields: Imaging of the NO Molecular Beam Splitting

J. O. Cáceres, M. Morato, and A. González Ureña*

Unidad de Láseres y Haces Moleculares, Instituto Pluridisciplinar, Universidad Complutense de Madrid, Madrid 28040, Spain

Received: October 17, 2006; In Final Form: November 16, 2006

The interaction between a NO supersonic beam and a resonant radio frequency (RF) field is investigated using laser ionization coupled to imaging techniques. It is shown how the resonant interaction leads to a beam splitting of ± 0.2 degrees toward both positive and negative direction perpendicular to the beam propagation axis. This phenomenon is rationalized using a model based on molecular interferences produced by the action of the resonant RF electric field.

Introduction

The interaction of a NO molecular beam with resonant radio frequency (RF) electric fields is a subject currently investigated by our group using different experimental methodologies.^{1–4} Thus depletion spectra of such polar molecular beams have been reported when the NO molecules interact with static and resonant RF fields.^{1–3} More recently⁴ deflection of 0.5° of a supersonic NO beam seeded in He was reported as a result of its resonant interaction with a RF electric field. It was shown that the formerly observed beam depletion¹ was the consequence of the beam deflection under resonant conditions.⁴ Though a full theoretical analysis of this phenomenon is still needed, recent work from our group^{5,6} indicated that the observed molecular beam deflection can be explained by molecular interferences.

In this Letter we further explore this phenomenon using a different experimental method, that of ion imaging technique. In ref 4 the beam profile was recorded by measuring the beam intensity as a function of the transverse position of a movable slit, but here the beam is ionized by one single laser pulse and the transverse profile monitored by an ion imaging detector. This new experimental approach was conceived as a way to investigate the resonant deflection phenomenon under better conditions, e.g., a better signal-to-noise ratio with spatial resolution and without the broadening effect of the beam slit.

We anticipate that the new results obtained in the present investigation can be rationalized by the onset of molecular interferences. Although atomic beam interferometry is well developed,⁷ there are not many examples of molecular beam interference in the literature.^{8–10} Up to now only a few types of molecular interferometers have been demonstrated. For example: a Ramsey–Bordé interferometer using I_2 ,⁸ a mechanical Mach–Zehnder interferometer for Na_2 ,⁹ and a Talbot–Lau interferometer for C_{70} fullerene molecules.¹⁰ The present work and results indicate that our experimental setup represents a novel method to investigate matter–wave interferences in molecular beams of polar molecules. As a matter of fact, our

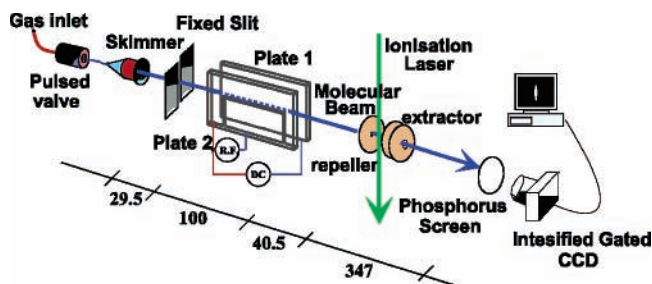


Figure 1. Schematic view of the molecular beam apparatus. The NO beam passes through the resonant unit and is subsequently ionized and detected by a phosphorus screen–CCD detector. All dimensions are in millimeters.

results seem to be, to the best of our knowledge, the first time that an image of molecular beam interferences is reported.

Experimental Method

Figure 1 shows a schematic view of the imaging molecular beam technique. The main features of the experimental methodology have been described elsewhere⁴ and only a brief description is given here. The present experiment employs the same NO beam (80% diluted in He) as used in ref 1. The resonance unit is of the same type described earlier.⁴ Essentially, it consists of two parallel Cu coated glass plates (length 10 cm along the beam, height 6 cm) separated by 0.67 cm. In one plate a 1 mm wide scratch insulates electrically a rectangle of 8 cm by 3 cm; the rectangle and the rest of the plate form the electrodes to which the RF is applied. The static voltage is applied to the rectangular electrode and the opposite plate. The molecular beam runs parallel to the scratch (along the x -axis) 0.34 cm away from the plate. At this distance the homogeneous static field (z -axis) is perpendicular to the RF field (y -axis). To monitor the beam profile, an imaging detector was used. The detector is a dual MCP-Phosphorus screen Hamamatsu-Photonics F2225-21P20 detector, coupled with an intensifier CCD camera Eureka Messtechnik GMBH-NFBV. Further experimental conditions are the same as used in our previous work.⁴

* Corresponding author. E-mail: laseres@pluri.ucm.es.

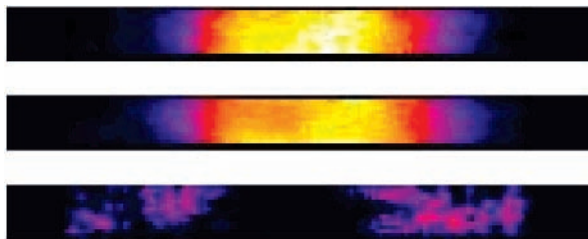


Figure 2. Three NO beam profile images; each one corresponds to 2.5×0.2 mm slice, false color is employed such that the blue/dark represents little or no beam signal and white the highest signal. The top image corresponds to “off” conditions, the middle one to “on” conditions and the bottom one to the “on” – “off” difference. Stagnation pressure was 2.8 bar. See text for comments.

The experimental procedure was the following: First, a static dc field of 1.47 kV/m was set into the two plates of the electric unit to produce a Stark splitting of 157 kHz for the NO $J = 3/2$ and $\Delta M = \pm 1$ transitions. Second, a resonant RF field of $\nu_{\text{on}} = 157$ kHz was established in between the RF plates. The gradient of the RF field at the center of the beam was determined to be 408.86 kV/m². Third, an image of the beam was taken by laser ionization under space focusing conditions;^{11,12} i.e., except for a magnification factor, the image reflects the beam profile at the ionization region right after it passed the resonant unit. In view of the beam deflection observed along the horizontal direction (i.e., perpendicular to the beam axis), it would have been more appropriate to send the laser beam horizontal rather than vertical. Unfortunately, it has not been possible for technical restrictions in the ionization chamber design. Nevertheless, the experimental resolution is good enough to observe the expected phenomenon. Work is in progress to implement this change in the laser beam configuration and makes it available in future investigations. Finally, conditions were varied to turn the RF field to off resonance, $\nu_{\text{off}} = 140$ kHz, and the corresponding image was taken, the rest of conditions being the same as those for the “on” image. A typical run consisted of averaging 100 laser shots for each “on” and “off” image.

Results

Figure 2 displays a composition of three images, each one corresponding to a horizontal slice of 2.5×0.2 mm, centered on the middle of the beam. False color is employed such that the blue/dark color represents little or no beam signal and white the highest signal. The top image corresponds to “off” conditions, the middle one to “on” conditions, and the bottom one to the “on” – “off” difference. Overall, the total accumulated signal of the “on” and “off” images are, within experimental errors, the same. Clearly, the bottom figure demonstrates how the effect of the resonant RF field is to split the beam toward both sides of the transverse direction.

A more quantitative display of this “on” – “off” profile is depicted in Figure 3. In this figure, the x -axis values represent the horizontal distance perpendicular to the beam propagation axis and the y -axis values denote the vertically averaged pixel intensity converted to percentage of NO intensity, normalized by the OFF maximum intensity profile. Notice that as a result of the resonant RF field a central part of the beam is deflected about $\pm 0.2^\circ$. Overall, the intensity of the missing central part, responsible for the depletion spectra in previous investigations when a fixed collimator was located in the beam direction, matches the two positive wings appeared at both sides of the beam.

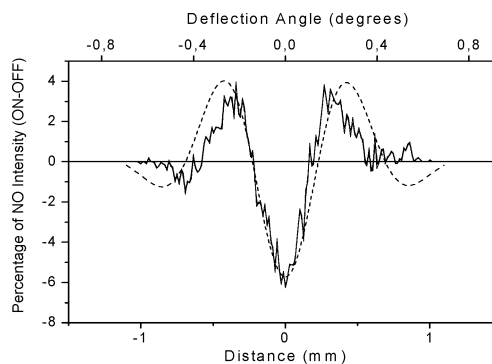


Figure 3. “ON–OFF” beam profile. Solid line corresponds to the experimental value and dashed line represents the calculated value given by $S^*(\text{on}) - S^*(\text{off})$. ON and OFF stand for the NO signal measured at 157 and 140 kHz conditions, respectively.

Discussion

The first point we mention is that the gradient of the RF field cannot explain the observed splitting of a few tenths of a degree. At the present experimental conditions, the largest force conceivable in the framework of electrostatic interaction can be written as $F < -\mu_z d/d_z(E_1)$ where μ_z is the mean z -component of μ , the molecular dipole moment and $d/d_z(E_1)$ is the gradient of the RF field. The maximal deflection angle is then given by $\theta_{\text{max}} = FL/(2E_{\text{tr}})$. With $L = 0.08$ m (the length of the interaction region), $E_{\text{tr}} \approx 0.1$ eV (the mean translational energy of NO), $d/d_z(E_1) = 408.86$ kV/m², and $\mu_z = \mu$, one obtains $\theta_{\text{max}} < 10^{-4}^\circ$, a value that is by orders of magnitude too small with respect to the observed one. Thus the RF gradient force acting on a free molecule cannot be responsible for the observed deflection angle of ca. 0.2° .

In previous work from our group,⁶ a model based on molecular interferences was developed to account for the observed beam profile. In the following a brief description of the model is presented. The reader is addressed to ref 6 for more details.

The resonant unit made by the static dc field and the resonant RF field can be considered as a simple closed two–arm interferometer⁷ of Ramsey type in which the two radio frequency zones, located at the entrance and exit of the unit, act as beam dividers. In these regions the RF fields induce transitions among the Stark levels split by the dc field as in a classic Ramsey separated oscillatory fields setup.^{13,14} Between the beam dividers the “phase object”⁷ consists of a RF electric field. The first RF field creates a coherent superposition of the two (J, M) Stark sublevels, and the second region re-superposes the outgoing wave before the molecular beam is detected. The phase object of the interferometer is the RF field created by the horizontal scratch along the beam propagation direction. This field creates under resonant conditions a distinct interaction potential on the different arms, i.e., on the distinct M_1 and M_2 states, and consequently, a phase shift is introduced between these two states. As a result, the interference is frozen and its pattern is observed by scanning the phase difference accumulated in between the two separated RF field dividers. In the present investigation the entire beam profile is measured by the imaging detector.

An important result of our model⁶ was that the normalized beam signal, S^* , is given by

$$S^* = \frac{1 - \cos \phi}{1 - \cos \phi_0} \quad (1)$$

Here ϕ is the extra phase shift introduced by the RF field and

ϕ_0 that of on resonant conditions. Essentially, the phase shift is given by the Glauber formalism¹⁵ as

$$\phi = -\frac{1}{\hbar v} \int_0^L W_{\text{stark}} dx \quad (2)$$

Here W_{stark} is the Stark energy for $M = 1$, v is the particle velocity along the beam propagation (x -axis) direction, and L is the length of the resonant unit. Details how to calculate the phase shift are given in ref 6.

Figure 3 also displays the calculated $S^*(\text{on}) - S^*(\text{off})$ values as a function of z , the perpendicular direction to the beam path. The calculation was done using eq 1 and the field given by $E_z = 0.75061 \text{ kV/m} - z \cdot 408.86 \text{ kV/m}^2$ (z is in meters). The latter corresponds to the experimental E_z field determined by a simulation¹⁶ using the experimental conditions. The agreement between the experimental and theoretical beam profiles displayed in Figure 3 is very satisfactory, demonstrating that the interferences created by the central resonant RF field are responsible for the observed beam splitting. For the calculation, the velocity spread of the beam was taken into account. Of relevance to the present work we should mention that the modulated transverse profile of a metastable argon atom beam was observed by Stern–Gerlach interferometry¹⁷ using a multichannel electron multiplier followed by a phosphor screen coupled to a CCD camera.

The difference of the present work with respect to that of ref 17 is multiple. In the first place, one should note the use of a molecular NO beam instead of an argon atomic beam. We think the present results constitute the first observation of molecular interferences using imaging techniques. Another main difference with respect to the cited work is the experimental setup that employs electric instead of magnetic fields. The present experimental methodology employs an oscillating RF field configuration as “phase object”. All these new ingredients open the way to get new insights in the study of molecular structure and spectroscopy using matter–wave interferometry.

Conclusions

This work has been dedicated to investigating the interaction of a supersonic NO beam with resonant oscillating RF electric fields using the ion imaging technique to measure the beam profile. The measurements clearly demonstrate how the interaction of a resonant RF field with the polar NO molecule produces a beam splitting of ± 0.2 degrees when the RF field gradient is 408.86 kV/m^2 .

One of the most relevant conclusions of the present investigation is that the phenomena observed in the present investigation can be explained by the occurrence of molecular interferences.

It is interesting to remark that the employed resonant electric unit, a simple device widely used in early molecular beam electric resonance experiments,¹⁸ seems to be adequate to investigate the matter wave behavior. Therefore the present approach is an original one and could offer new possibilities and applications in molecular interferometry.

Acknowledgment. Financial support from the Ministerial de Educación y Ciencia of Spain (grant CTQ2004-3468) is gratefully acknowledged. J.O.C. acknowledges a Ramón y Cajal Research Contract from The Ministerio de Educación y Ciencia of Spain. We thank Dr. Skowronek for his technical assistance and design of the imaging detector chamber. The imaging analysis shown in this work was performed with the ImageJ program. We acknowledge this facility and free software obtained from Rasband, W.S., ImageJ, National Institutes of Health, Bethesda, Maryland, <http://rsb.info.nih.gov/ij/>, 1997–2004.

References and Notes

- (1) Montero, C.; González Ureña, A.; Caceres, J. O.; Morato, M.; Najera, J.; Loesch, H. J. *Eur. Phys. J. D.* **2003**, *26*, 261.
- (2) Morato, M.; Gasmi, K.; Montero, C.; González Ureña, A. *Chem. Phys. Lett.* **2004**, *392*, 255.
- (3) Caceres, J. O.; Montero, C.; Morato, M.; González Ureña, A. *Chem. Phys. Lett.* **2006**, *426*, 214.
- (4) Morato, M.; Caceres, J. O.; González Ureña, A. *Eur. Phys. J. D* **2006**, *38*, 215.
- (5) Morato, M.; Caceres, J. O.; González Ureña, A. *Eur. Phys. J. D* **2006**, *39*, 199.
- (6) González Ureña, A.; Caceres, J. O.; Morato, M. *Chem. Phys.* **2006**, *328*, 156.
- (7) Baudon, J.; Mathevet, R.; Robert, J. J. *Phys. B: At. Mol. Opt. Phys.* **1999**, *32*, R173.
- (8) Bordé, C.; Coutier, N.; Burck, F. D.; Goncharov, A.; Gorlicki, M. *Phys. Lett. A* **1984**, *188*, 187.
- (9) Chapman, M. S.; Ekstrom, C. R.; Hammond, T. D.; Rubenstein, R. A.; Schmiedmayer, J.; Wehinger, S.; Pritchard, D. E. *Phys. Rev. Lett.* **1995**, *74*, 4783.
- (10) Brezger, B.; Hackermuller, L.; Utterthaler, S.; Petschinka, J.; Arndt, M.; Zeilinger, A. *Phys. Rev. Lett.* **2002**, *88*, 100404.
- (11) Chandler, D. W.; Houston, P. L. *J. Chem. Phys.* **1987**, *87*, 1445.
- (12) Parker, D. H.; Eppink, A. T. J. B. Velocity mapping in applications in molecular dynamics and experimental aspects. In *Imaging in molecular dynamics: Technology and applications – A user guide*; Whitaker, B. J., Ed.; Cambridge University Press: Cambridge, U.K., 2003; p 20.
- (13) Ramsey, N. F. *Phys. Rev.* **1950**, *78*, 695.
- (14) Ramsey, N. F. *Molecular Beams*; Oxford University Press: Oxford, U.K., 1965.
- (15) Glauber, R. J. *Lectures in Theoretical Physics*; Interscience: New York, 1959; Vol. 1.
- (16) The calculation was done using the Simion 7.0 programme.
- (17) Viaris de Lesegno, B.; Karma, J. C.; Boustimi, M.; Perales, F.; Mainos, C.; Reinhardt, J.; Baudon, J.; Bocvarski, V.; Grancharova, D.; Pereira Dos Santos, F.; Durt, T.; Haberland, H.; Robert, J. *Eur. Phys. J. D* **2003**, *23*, 25.
- (18) Trischka, J. W. *Phys. Rev.* **1948**, *74*, 718.